increasing energy, starting with the ground state. The dashed line was required to pass through the origin and was least-squares fitted to the crosses 0, 1, 2, and 4. The proportionality between $(2I+1)$ and these cross sections is excellent with a nominal rms deviation of 6.5%. The spin and parity of the third excited state were previously thought to be $\frac{7}{2}^-$,[30] but more recent studies strongly imply a $\frac{5}{2}^-$ assignment.[32–35] A direct application of the $(2I+1)$ rule would yield the apparently incorrect $\frac{3}{2}$ spin value. Under the assumption that the angular distributions are incoherent superpositions of isotropic SCN and nonisotropic DI contributions as described in detail in Sec. III-A, the proportionality between the SCN component of the cross sections and $(2I+1)$ may be investigated. This analysis is also shown in Fig. 2 where the solid circles represent the SCN contributions to the cross sections. The solid line was required to pass through the origin and was least-squares fitted to the five cross sections represented by the solid circles. The argreement is good for all cross sections (rms deviation 14.6%) including the one which had appeared anomalous in the previous treatment. While the validity of this type of decomposition can be seriously challenged, the over-all agreement with the $(2I+1)$ rule of SCN theory is improved considerably. It would be interesting to investigate whether such improvement would result for other (d,α) reactions under similar analysis.

ACKNOWLEDGMENTS

The authors would like to express their gratitude to F. Hobaugh and K. Runck for their unstinting efforts in the operation and maintainence of the cyclotron throughout the execution of this investigation.

PHYSICAL REVIEW VOLUME 138, NUMBER 1B 12 APRIL 1965

Elastic Electron Scattering from Tritium and Helium-3*

H. COLLARD, R. HOFSTADTER, E. B. HUGHES, A. JOHANSSON,† AND M. R. YEARIAN
Department of Physics and High-Energy Physics Laboratory, Stanford University, Stanford, California

AND

R. B. DAY AND R. T. WAGNER‡
Los Alamos Scientific Laboratory, University of California, Los Alamos, New Mexico

(Received 23 November 1964)

The mirror nuclei of tritium and helium-3 have been studied by the method of elastic electron scattering. Absolute cross sections have been measured for incident electron energies in the range 110–680 MeV at scattering angles lying between 40 and 135° in this energy range. The data have been interpreted in a straightforward manner and form factors are given for the distributions of charge and magnetic moment in the two nuclei over a range of four-momentum transfer squared 1.0–8.0 F^{-2}. Model-independent radii of the charge and magnetic-moment distributions are given and an attempt is made to deduce form factors describing the spatial distribution of the protons in tritium and helium-3.

INTRODUCTION

ONE of the important questions in nuclear physics concerns a problem about which we are almost totally ignorant; this is the question of whether significant three-body nuclear forces exist.[1] The obvious place to search for evidence of such forces is in the simplest nuclei in which they can occur—tritium and helium-3. However, despite a growing body of experimental data on these nuclei, as well as on scattering and reactions of protons and neutrons with deuterons, we still do not have enough information to provide an insight into the details of the structure of the three-body systems. For example, Blatt[2,3] and his collaborators have made a determined effort to calculate the binding energy of the triton by a variational type of calculation in which the best-known parameters of the two-body nuclear forces were used. Their difficulty in obtaining reasonable agreement with the experimental binding energy can be ascribed partly to uncertainties in our knowledge of the two-body forces as well as to the lack of a suitable trial wave function. Thus, data that will improve our knowledge of the ground-state wave functions would be particularly helpful. If, when better

* This work was supported in part by the U. S. Office of Naval Research, the U. S. Atomic Energy Commission, and the U. S. Air Force Office of Scientific Research.

† Present address: Gustaf Werner Institute, Uppsala University, Uppsala, Sweden.

‡ Present address: Department of Physics, St. Mary's College, Winona, Minnesota.

[1] V. F. Weisskopf, in *Proceedings of the International Conference on Nuclear Structure, Kingston,* edited by D. A. Bromley and E. W. Vogt (University of Toronto Press, Toronto, 1960), p. 890.

[2] J. M. Blatt, G. H. Derrick, and J. N. Lyness, Phys. Rev. Letters 8, 323 (1962).

[3] J. M. Blatt and L. M. Delves, Phys. Rev. Letters 12, 544 (1964).

two-body forces and improved wave functions are available for calculations such as Blatt's, there remains a discrepancy between the calculated result and experiment, one might then begin to look for the origin of the discrepancy in three-body forces. At the present time, however, our knowledge of the experimental facts is not sufficiently detailed to permit a definitive answer to be made to the question of three-body forces.

Since past experience has shown that the results of high-energy electron scattering experiments can often reveal more about the details of the ground state of a nucleus than can nucleon scattering, we have investigated in some detail the elastic scattering of electrons on tritium and helium-3. This paper describes an experiment in which the cross sections for elastic electron scattering by these nuclei have been measured. Since the comparison method that has been used tends to minimize most systematic errors, the relative accuracy of the cross sections is determined mostly by counting statistics (of the order of a few percent), while the absolute accuracy is determined principally by the precision with which the scattering for the proton is known.

In preliminary accounts of this experiment, experimental data were given and an attempt was made to analyze the electromagnetic form factors obtained from the elastic-scattering results in terms of the body form factors of the nuclei and the charge form factor of the neutron.[4–6] However, further investigation by Schiff and others shows that the preliminary analysis used there is inadequate in several ways.[7–14] Furthermore, the values for the neutron charge form factor that are obtained from our latest results on tritium and helium-3 are negative and in disagreement with those obtained from other measurements[15–18] by an amount probably outside experimental error. In view of these difficulties and because the theory is presently being improved, we have confined ourselves to presenting the charge and magnetic form factors that are derived from the experimental cross sections and to analyzing these in terms of the spatial distribution of the protons within the two nuclei.

EXPERIMENTAL METHOD

The scattering targets used in this experiment consisted of high-pressure gas targets of tritium, helium-3, and hydrogen. The target cells, which were cylinders with hemispherical end caps, were made as nearly identical as possible in order to eliminate possible systematic errors in measuring the relative cross sections. The over-all length was 7.68 in. and the outside diameter was 0.75 in. The cylindrical section had a wall thickness of 0.020 in., while that of the hemispherical end caps was 0.010 in. The various parts were joined together by an electron-beam welding process, which provided a strong joint that showed no indication of leaks in a properly made weld.

Since the tritium targets contained as much as 25 000 curies of activity, an extensive testing program was undertaken to ensure that the cells would not leak or break. All parts were nondestructively tested by several methods to make sure that no flaws existed that might lead to failure of the cells. Following assembly, the cells were radiographed and leak-tested. Several typical cells were then subjected to pressure tests to measure the pressure at which the yield point and final rupture occurred. If these agreed with the design calculations, the rest of the cells were considered acceptable. However, before being filled, all cells were proof-tested at a pressure 50% higher than the anticipated filling pressure. In general, the filling pressure was approximately half the pressure at which the yield point occurred and about 38% of the breaking pressure.

Two different types of stainless steel were used which tests had shown not to be embrittled by hydrogen at room temperature. The earlier target cells were made of type 304 stainless steel and were filled to a pressure of 1500 psi. Later cells were fabricated of type A-286 stainless steel. This material was heat-treated to increase its strength; thus the A-286 cells could be filled to 3000 psi. The filling was done through a stainless-steel capillary tube that had been hard soldered to the target cell. After filling, the capillary was pinched off and welded in a single operation. The largest leak rate observed in a tritium cell corresponded to a loss of only one atmospheric cc in 10^4 years from a 1500-psi filling. However, this figure is an upper limit since the tritium observed may have been coming from a trapped pocket in the capillary weld. Although all the cells used at any one time were filled to very nearly the same pressure, it was necessary to use an accurate equation of state for each gas in order to obtain the nuclear density. In addition, the tritium results were corrected for the

[4] H. Collard, R. Hofstadter, A. Johansson, R. Parks, M. Ryneveld, A. Walker, M. R. Yearian, R. B. Day, and R. T. Wagner, Phys. Rev. Letters **11**, 132 (1963).
[5] L. I. Schiff, H. Collard, R. Hofstadter, A. Johansson, and M. R. Yearian, in *Proceedings of the International Conference at Stanford University, 1963* (Stanford University Press, Palo Alto, California, 1964), p. 385.
[6] L. I. Schiff, H. Collard, R. Hofstadter, A. Johansson, and M. R. Yearian, Phys. Rev. Letters **11**, 387 (1963).
[7] L. I. Schiff, Phys. Rev. **133**, B802 (1964).
[8] A. Johansson, Phys. Rev. **136**, B1030 (1964).
[9] T. A. Griffy and R. J. Oakes, Phys. Rev. **135**, B1161 (1964).
[10] T. A. Griffy, Phys. Letters **11**, 155 (1964); K. Okamoto, *ibid.* **11**, 150 (1964).
[11] N. T. Meister, T. K. Radha, and L. I. Schiff, Phys. Rev. Letters **12**, 509 (1964).
[12] L. I. Schiff, R. J. Oakes, T. K. Radha, N. T. Meister, B. F. Gibson, B. P. Carter, and T. A. Griffy, International Conference on High-Energy Physics at Dubna, 1964 (to be published).
[13] A. Q. Sarker, Phys. Rev. Letters **13**, 375 (1964).
[14] D. A. Kreuger and A. Goldberg, Phys. Rev. **135**, B934 (1964).
[15] J. S. Levinger and T. L. Chow, Bull. Am. Phys. Soc. **9**, 465 (1964).
[16] E. B. Hughes, T. A. Griffy, M. R. Yearian, and R. Hofstadter, International Conference on High-Energy Physics at Dubna, 1964 (to be published).
[17] C. de Vries, R. Hofstadter, A. Johansson, and Robert Herman, Phys. Rev. **134**, B848 (1964).
[18] D. Drickey, B. Benaksas, and D. Frerejacque, Bull. Am. Phys. Soc. **9**, 379 (1964).

helium-3 growing in from the tritium decay as well as for the small amounts (1–2%) of hydrogen and deuterium that were present. The helium-3 and hydrogen cells always contained a negligible amount of impurities.

The high-energy electron beam, with an energy spread of about 1%, was supplied by the Stanford Mark III linear accelerator. The incident electron beam, which had a diameter of 0.25 in., could usually pass along the axis of the cylindrical target without striking the side walls. However, in some cases the multiple scattering from the entrance wall of the target cell was sufficient to cause a small amount of scattering to occur from the side walls. The amount of this scattering was usually negligible but could be determined by measuring the counting rate at a scattered electron energy above that of the elastic peak.

The electrons scattered from the target gas were analyzed in momentum by a 72-in. double-focusing 180° spectrometer. The optics of the spectrometer, together with the scattering angle, defined the gas volume in which scattering could be observed. The scattered electrons were detected by an array of ten plastic scintillation counters located at the image plane of the spectrometer. These detectors were divided into two groups of five counters, with each group being operated in coincidence with a large fluorochemical Čerenkov counter placed behind it. Each detector channel covered a momentum interval of 0.37%. Thus, at a single setting of the magnetic field, one could measure a spectrum extending over an interval of about 3.7% in momentum.

An accurate knowledge was required of the relative detection efficiencies of the various detector channels. The efficiencies were determined by measuring the quasielastic spectrum from a carbon target in a region where the spectrum is slowly varying. By taking a number of overlapping spectra and treating the data appropriately, one can obtain the relative channel efficiencies without an *a priori* knowledge of the momentum variation of the spectrum.

Spectra in the region of the elastic scattering peak were measured for all three nuclei for values of the square of the momentum transfer q^2 in the range 1.0–8.0 F^{-2}. At each value of q^2 the measurements were

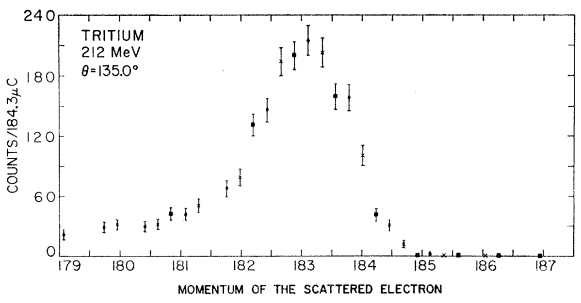

FIG. 1. A typical elastic cross section plotted as a function of scattered electron momentum in MeV.

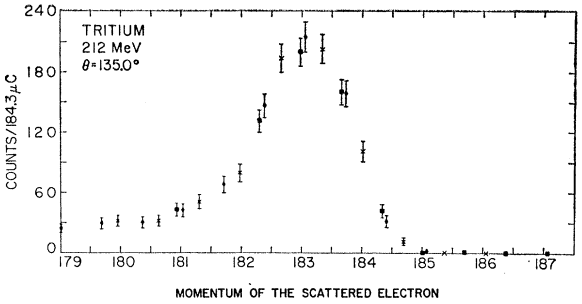

FIG. 2. The data of Fig. 1 after application of the small peak-shifting operation.

made for at least three scattering angles between 40 and 135°. By referring these measurements to the known scattering properties of the proton, it was then possible to deduce the cross sections and form factors for tritium and helium-3. A detailed knowledge of target thickness, the effective solid angle of the spectrometer, and the absolute efficiencies of the detector channels was thus not required since the measurements for the three nuclei were made under almost identical conditions.

In the measurements of the scattered electron spectra, the momentum spread of each detection channel was often large enough so that the width of the elastic peak would be only a few channels. To obtain a better measurement of the shape of this peak, we took at least three overlapping spectrum measurements with the field shifted by the equivalent of one-third channel each time. Typical data are shown in Fig. 1. There, the counts for four spectrometer settings (distinguished in the plot by different plotting symbols) are displayed as a function of scattered electron momentum. The counts have been corrected for counting rate losses and for the slight variations in relative channel efficiencies. In some cases it was obvious from the shape of the spectra that the change in the field had not been exactly what we had intended. In these cases we have made arbitrary but small shifts in the spectra in order to smooth out the peak. The result of applying this procedure to the data of Fig. 1 is shown in Fig. 2. The improved peak shape is apparent. Such shifts have little effect on the cross section. In this particular case the correction was such as to decrease the observed cross section by 0.7%, and usually the correction was less than 1%.

The length of each run was monitored by collecting the electron beam in a Faraday cup and integrating the charge in a current integrator with an accuracy of 0.1%. In addition, the position of the beam was checked by occasionally observing its position on a zinc sulfide screen that could be inserted into the beam. Since only relative measurements were required, it was not necessary to know the absolute collection efficiency of the Faraday cup for this experiment.

The following corrections were applied to the measured spectra in addition to the one just mentioned:

(1) Counting rate losses. These were treated in a

standard manner[19] and always amounted to less than 5%.

(2) Relative channel efficiencies. The manner in which these efficiencies are determined has already been explained. Channel-to-channel variations in the efficiencies were never greater than 5%.

(3) Bremsstrahlung effects. The electron spectrum is affected by electron radiation both during the scattering process and during passage through the target and target cell. Corrections for this process were made following Tsai's theory according to the computer program of Crannell[19] in which the radiation effects are unfolded from the spectrum. It is worthwhile noting that the bremsstrahlung correction was not important because of the manner in which the data were taken. Thus, only the differences in radiative scattering (arising from the different recoil energies of the proton and the two heavier nuclei) were important. These were of the order of 0.1% or less.

(4) Resolution. At the higher energies, the experimental resolving power was not sufficient to produce a complete resolution of the elastic peak from the continuum due to inelastic scattering. Such a case is shown in Fig. 3. However, after the corrections enumerated above had been made, it was possible to extrapolate the inelastic continuum smoothly into the region under the elastic peak and then subtract this contribution from the elastic peak. In Fig. 4, the data of Fig. 3 are shown after the effects of electron radiation were unfolded. The smooth curve represents the estimated contribution from the inelastic continuum which was then subtracted from the elastic peak.

(5) Tritium decay. The tritium spectra had to be corrected for growth of helium-3 in the target cell that resulted from the tritium decay. Since the tritium was purified by passing it through a palladium leak just before filling the cell, and the filled cells were not used longer than six months, the maximum helium-3 contamination in the tritium was 3%.

After these corrections were made, the number of counts was normalized to the density of nuclei in the target. This number, which is proportional to the elastic-scattering cross section, was then used in the analysis described in the next section.

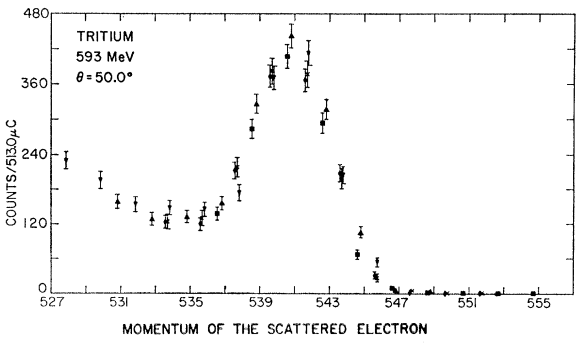

FIG. 3. An example of an elastic peak incompletely resolved from the tail of the inelastic scattering peak.

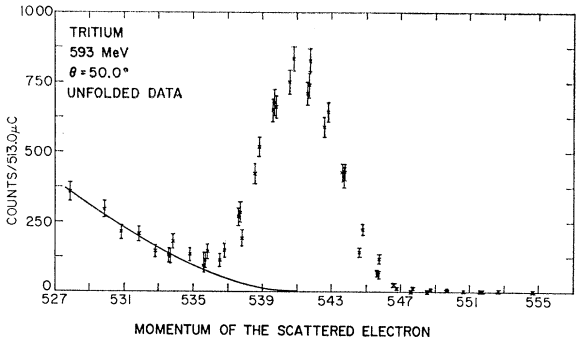

FIG. 4. The data of Fig. 3 after the effects of electron radiation have been unfolded. The smooth curve represents the estimated contribution from the inelastic continuum.

ANALYSIS

Since the proton, triton, and helium-3 all have spin $\frac{1}{2}\hbar$, the elastic scattering cross section for these three nuclei can be described by the Rosenbluth formula (in units where $\hbar=c=1$)

$$\frac{d\sigma}{d\Omega}=\sigma_{\mathrm{NS}}\left\{F_{\mathrm{ch}}^2(q^2)+F_{\mathrm{mag}}^2(q^2)(1+K)^2\frac{q^2}{4M^2}\times\left[1+2\left(1+\frac{q^2}{4M^2}\right)\tan^2\left(\frac{\theta}{2}\right)\right]\right\}\Big/\left(1+\frac{q^2}{4M^2}\right),$$

where

$$\sigma_{\mathrm{NS}}=\left(\frac{Ze^2}{2E}\right)^2\frac{\cos^2(\theta/2)}{\sin^4(\theta/2)}\frac{1}{1+(2E/M)\sin^2(\theta/2)}. \quad (1)$$

E=incident energy of electron in laboratory system, q=the four-momentum transfer, M=the mass of the scattering nucleus, Z=the charge of the scattering nucleus, $F_{\mathrm{ch}}(q^2)$=the charge form factor, normalized to unity at $q^2=0$, $F_{\mathrm{mag}}(q^2)$=the magnetic form factor, normalized to unity at $q^2=0$, K=the anomalous nuclear magnetic moment expressed in magneton units related to the scattering nucleus, i.e., $K=1.79$ for the proton, $K=7.94$ for the triton, $K=-4.20$ for helium-3.

The data obtained for each value of q^2 were analyzed in such a way as to yield those charge and magnetic form factors for tritium and helium-3 which minimized the statistical function χ^2 defined as

$$\chi^2=\sum_l\sum_i\frac{(\sigma_{l,i}-C_lX_{l,i})^2}{C_l^2(\Delta X_{l,i})^2},$$

where the index l refers to the scattering angle and the index i to the target. The cross sections $\sigma_{l,i}$ were found from Eq. (1), using the proton form factors found by

[19] H. L. Crannell, thesis, Stanford University, Stanford, California, 1964 (unpublished).

de Vries *et al.*[17] (combination b'), and trial form factors for tritium and helium-3. The quantities $X_{l,i}$ are the normalized number of counts in the elastic peaks after the various corrections described above have been applied. The errors $\Delta X_{l,i}$ have been assumed to arise from counting statistics alone. The normalization constants C_l are also to be determined in such a way that χ^2 attains its minimum value. They can be eliminated from the expression for χ^2 by equating the derivatives of χ^2 with respect to C_l to zero.

Then, with the definitions

$$T_{l,i}=\sigma_{l,i}/\Delta X_{l,i} \quad \text{and} \quad E_{l,i}=X_{l,i}/\Delta X_{l,i},$$

we obtain

$$C_l=\sum_i T_{l,i}^2/\sum_i T_{l,i}E_{l,i}$$

and

$$\chi^2=\sum_l \{\sum_i \sum_{j>i} (T_{l,i}E_{l,j}-T_{l,j}E_{l,i})^2/\sum_i T_{l,i}^2\}$$

with

$$N=(\sum_l \sum_i 1)-(\sum_l 1)-4 \text{ degrees of freedom.}$$

This expression for χ^2, at a particular value of q^2, depends only on the value of the charge and magnetic form factors of tritium and helium-3. These parameters are automatically adjusted, using an IBM 7090 computer, until a minimum value of χ^2 is found. The normalization constants C_l are computed at the same time; hence one obtains the set of experimental cross sections which together with the final set of form factors generates the minimum value of the function χ^2.

RESULTS AND DISCUSSION

The experimental cross sections obtained as described in the last section are given in Table I.

Table II gives the charge and magnetic form factors of tritium and helium-3 that produce the best fit to the data. The errors in these quantities were computed from the error matrix, which was also calculated by the computer. The quoted errors have been based on external or internal consistency, depending upon which gave the larger uncertainty. The final column in Table II shows the goodness of fit. At all values of q^2, with the exception of $q^2=8$ F^{-2}, the value of χ^2/N is larger than unity, which is to be expected since only the rather small errors arising from counting statistics have been considered in this computation. The deviations from unity of χ^2/N are not sufficient to indicate a failure of the Rosenbluth formula.

In Fig. 5 we show the variation of the charge form factor of helium-3 with the square of the four-momentum transfer q^2. For the sake of comparison the other form factors are given in Fig. 6 in the form of ratios of form factors. Several conclusions can be drawn from these ratios:

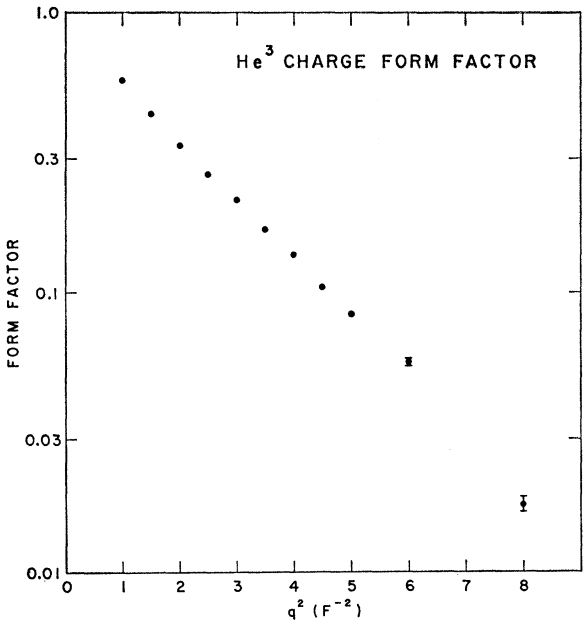

FIG. 5. The charge form factor of helium-3 as a function of four-momentum transfer squared.

(a) The charge and magnetic form factors of tritium are very similar, with the exception of the point at $q^2=8$ F^{-2}.

(b) The charge form factor of helium-3 is significantly smaller than the magnetic form factor, although the effect is not quite as marked as was originally suggested by the data of Collard and Hofstadter.[20]

(c) Both the charge and magnetic form factors of tritium decrease less rapidly with increasing q^2 than the corresponding form factor in helium-3, suggesting that both the charge and magnetic radii of tritium are smaller than in helium-3.

The theory of the magnetic form factors of tritium and helium-3 given by Schiff[7] cannot be used without modification to extract information about the three-body wave function unless the contributions due to meson exchange and Coulomb effects, etc., are included. However, with the assumptions that the nuclei of tritium and helium-3 can be described by three-nucleon wave functions and that the charge form factors of these nucleons are given by the free nucleon form factors, the charge form factors of tritium and helium-3 can be written quite generally in the form[21]

$$F_{\rm ch}(\mathrm{He}^3)=F_{\rm ch}(p)F_L(\mathrm{He}^3)+\tfrac{1}{2}F_{\rm ch}(n)F_O(\mathrm{He}^3), \quad (2)$$

$$F_{\rm ch}(\mathrm{H}^3)=F_{\rm ch}(p)F_O(\mathrm{H}^3)+2F_{\rm ch}(n)F_L(\mathrm{H}^3), \quad (3)$$

where the form factors $F_L(\mathrm{H}^3)$ and $F_L(\mathrm{He}^3)$, describing the spatial distribution of like nucleons, and $F_O(\mathrm{H}^3)$ and $F_O(\mathrm{He}^3)$, describing the spatial distribution of the odd

[20] H. Collard and R. Hofstadter, Phys. Rev. **131**, 416 (1963).
[21] T. A. Griffy (private communication).

TABLE I. Absolute cross sections for the elastic scattering of electrons from hydrogen, tritium, and helium-3. The experimental errors are given as a percentage and are only statistical in nature.

θ(deg)[a]	E_0(MeV)	$\left(\frac{d\sigma}{d\Omega}\right)_{H^1}$[b]	$\left(\frac{\Delta d\sigma/d\Omega}{d\sigma/d\Omega}\right)_{H^1}$	$\left(\frac{d\sigma}{d\Omega}\right)_{He^3}$	$\left(\frac{\Delta d\sigma/d\Omega}{d\sigma/d\Omega}\right)_{He^3}$	$\left(\frac{d\sigma}{d\Omega}\right)_{H^3}$	$\left(\frac{\Delta d\sigma/d\Omega}{d\sigma/d\Omega}\right)_{H^3}$
$q^2=1.0$(F^{-2})							
40	291.9	3.25×10^{-30}	1.4	4.98×10^{-30}	1.4	1.68×10^{-30}	1.8
40	291.9			5.01×10^{-30}	2.1	1.69×10^{-30}	1.9
50	236.9	1.95×10^{-30}	1.7	3.02×10^{-30}	1.9		
60	200.8	1.27×10^{-30}	1.9	1.97×10^{-30}	2.1	6.77×10^{-31}	2.1
60	200.8	1.27×10^{-30}	3.5	1.95×10^{-30}	3.5		
80	157.0	5.83×10^{-31}	3.5	9.62×10^{-31}	3.4		
100	132.3	3.10×10^{-31}	1.5	4.74×10^{-31}	1.7	1.87×10^{-31}	1.8
120	117.4	1.78×10^{-31}	2.0	2.23×10^{-31}	2.5	1.06×10^{-31}	2.7
120	117.4	1.75×10^{-31}	4.2	2.26×10^{-31}	4.0		
135	110.3	1.13×10^{-31}	1.9	1.26×10^{-31}	3.3	7.38×10^{-32}	3.4
$q^2=1.5$							
40	358.5	1.97×10^{-30}	1.4	1.94×10^{-30}	1.6	7.42×10^{-31}	1.8
40	358.5			1.96×10^{-30}	1.8	7.34×10^{-31}	2.2
40	358.5	2.06×10^{-30}	3.1	1.86×10^{-30}	2.9		
50	291.2	1.19×10^{-30}	3.2	1.16×10^{-30}	3.2		
50	291.2	1.19×10^{-30}	1.6	1.17×10^{-30}	1.8		
60	246.9	7.61×10^{-31}	1.6	7.65×10^{-31}	1.7	3.06×10^{-31}	2.1
60	246.9	8.03×10^{-31}	2.8	7.32×10^{-31}	2.8		
80	193.3	3.84×10^{-31}	3.2	3.49×10^{-31}	3.2		
100	163.0	2.10×10^{-31}	3.8	1.73×10^{-31}	3.8		
120	144.8	1.15×10^{-31}	1.6	8.81×10^{-32}	2.0	5.13×10^{-32}	2.1
120	144.8	1.16×10^{-31}	3.4	8.85×10^{-32}	3.5		
135	136.1	8.31×10^{-32}	2.9	5.03×10^{-32}	2.9	3.43×10^{-32}	2.2
$q^2=2.0$							
40	414.9	1.39×10^{-30}	1.4	8.49×10^{-31}	1.4	3.42×10^{-31}	1.5
40	414.9			8.45×10^{-31}	2.0	3.50×10^{-31}	2.2
40	414.9	1.39×10^{-30}	3.1	8.29×10^{-31}	3.4		
50	337.2	8.51×10^{-31}	1.8	5.01×10^{-31}	1.6		
60	286.1	5.32×10^{-31}	1.6	3.38×10^{-31}	2.4	1.47×10^{-31}	2.5
60	286.1			3.30×10^{-31}	2.0	1.43×10^{-31}	2.2
60	286.1	5.43×10^{-31}	3.3	3.31×10^{-31}	3.3		
80	224.1	2.64×10^{-31}	1.7	1.55×10^{-31}	2.4	7.41×10^{-32}	2.5
80	224.1	2.77×10^{-31}	3.5	1.51×10^{-31}	3.3		
100	189.2	1.42×10^{-31}	3.0	8.21×10^{-32}	3.1		
100	189.2	1.42×10^{-31}	3.0	8.27×10^{-32}	3.2		
100	189.2	1.36×10^{-31}	4.0	8.40×10^{-32}	3.3		
120	168.2	8.46×10^{-32}	1.9	4.13×10^{-32}	2.7	2.69×10^{-32}	2.6
120	168.2	8.74×10^{-32}	4.0	4.01×10^{-32}	4.0		
135	158.1	6.16×10^{-32}	3.3	2.38×10^{-32}	3.2		
135	158.1	6.40×10^{-32}	1.8	2.24×10^{-32}	3.4	1.88×10^{-32}	2.6
$q^2=2.5$							
40	464.9	1.02×10^{-30}	1.9	4.08×10^{-31}	1.6	1.94×10^{-31}	1.9
40	464.9			4.18×10^{-31}	2.0	1.89×10^{-31}	2.1
40	464.9	1.09×10^{-31}	3.5	3.95×10^{-31}	3.3		
50	377.9	6.14×10^{-31}	1.6	2.58×10^{-31}	2.1	1.15×10^{-31}	2.2
60	320.8			1.66×10^{-31}	1.8	7.64×10^{-32}	1.9
60	320.8	4.00×10^{-31}	1.6	1.61×10^{-31}	2.1	8.05×10^{-32}	2.1
80	251.5			7.52×10^{-32}	3.2	4.13×10^{-32}	3.1
80	251.5	2.13×10^{-31}	3.4	7.20×10^{-32}	3.8		
100	212.5	1.10×10^{-31}	3.1	3.98×10^{-32}	3.0		
120	189.0	6.81×10^{-32}	1.4	2.00×10^{-32}	2.3	1.59×10^{-32}	2.2
135	177.7	5.02×10^{-32}	3.8	1.19×10^{-32}	3.9		
135	177.7	5.10×10^{-32}	1.9	1.18×10^{-32}	3.3	1.17×10^{-32}	2.5
$q^2=3.0$							
40	510.1	7.64×10^{-31}	1.3	2.28×10^{-31}	1.8	1.19×10^{-31}	1.7
40	510.1			2.27×10^{-31}	1.6	1.13×10^{-31}	1.7
40	510.1	8.49×10^{-31}	3.2	2.12×10^{-31}	3.1		
40	510.1	8.15×10^{-31}	2.9	2.18×10^{-31}	2.9		
50	414.9	4.86×10^{-31}	1.2	1.33×10^{-31}	1.3		
60	352.3			8.79×10^{-32}	2.0	4.65×10^{-32}	2.0
60	352.3	3.20×10^{-31}	2.9	8.57×10^{-32}	3.2		
60	352.3	3.20×10^{-31}	1.7	8.73×10^{-32}	2.2	4.59×10^{-32}	2.3
80	276.5			4.04×10^{-32}	3.3	2.45×10^{-32}	3.1
100	233.7	9.11×10^{-32}	1.5	2.05×10^{-32}	2.2	1.40×10^{-32}	2.3

[a] Because there are differences in value of the recoil momentum for the proton and the three-body nuclei at the same incident energy and angle, only the q^2 values for the three-body nuclei are quoted in the table.

[b] The proton cross sections were not measured absolutely in these experiments but were taken from the values given in Ref. 17 (combination b'). The errors in the proton cross sections in the fourth column are statistical errors.

TABLE I. (*continued*)

θ(deg)[a]	E_0(MeV)	$\left(\frac{d\sigma}{d\Omega}\right)_{H^1}$[b]	$\left(\frac{\Delta d\sigma/d\Omega}{d\sigma/d\Omega}\right)_{H^1}$	$\left(\frac{d\sigma}{d\Omega}\right)_{He^3}$	$\left(\frac{\Delta d\sigma/d\Omega}{d\sigma/d\Omega}\right)_{He^3}$	$\left(\frac{d\sigma}{d\Omega}\right)_{H^3}$	$\left(\frac{\Delta d\sigma/d\Omega}{d\sigma/d\Omega}\right)_{H^3}$
$q^2=3.0$							
100	233.7	8.89×10^{-32}	3.1	2.09×10^{-32}	3.2		
120	208.0	5.57×10^{-32}	1.6	1.07×10^{-32}	2.9	9.44×10^{-33}	2.6
120	208.0	5.61×10^{-32}	3.8	1.05×10^{-32}	4.0		
135	195.7	4.17×10^{-32}	3.1	6.23×10^{-33}	3.7		
135	195.7	4.23×10^{-32}	1.5	5.98×10^{-33}	3.1	7.08×10^{-33}	2.1
$q^2=3.5$							
40	551.9	6.26×10^{-31}	2.2	1.20×10^{-31}	2.1	6.65×10^{-32}	1.8
40	551.9			1.19×10^{-31}	1.9	6.66×10^{-32}	1.9
40	551.9	6.22×10^{-31}	3.1	1.21×10^{-31}	3.1		
50	449.0	3.81×10^{-32}	1.6	7.32×10^{-32}	1.9		
60	381.5			4.69×10^{-32}	2.2	2.73×10^{-32}	2.0
60	381.5	2.55×10^{-31}	1.5	4.55×10^{-32}	2.1	2.78×10^{-32}	1.5
80	299.5			2.18×10^{-32}	2.9	1.44×10^{-32}	2.6
80	299.5	1.34×10^{-31}	3.2	2.06×10^{-32}	4.2		
100	253.4	7.62×10^{-32}	1.6	1.05×10^{-32}	3.0	8.60×10^{-33}	2.5
100	253.4	7.84×10^{-32}	4.3	1.04×10^{-32}	5.2		
120	225.6	4.73×10^{-32}	2.1	5.69×10^{-33}	3.7	5.77×10^{-33}	2.5
120	225.6	4.50×10^{-32}	4.8	6.63×10^{-33}	6.9		
135	212.3	3.48×10^{-32}	4.1	3.81×10^{-33}	6.2		
135	212.3	3.60×10^{-32}	2.3	3.48×10^{-33}	3.0	4.46×10^{-33}	2.9
$q^2=4.0$							
40	590.9	5.08×10^{-31}	1.7	7.04×10^{-32}	2.7	4.11×10^{-32}	2.6
40	590.9			6.82×10^{-32}	1.5	4.03×10^{-32}	1.4
50	481.0	3.15×10^{-31}	1.2	4.14×10^{-32}	1.9		
60	408.8			2.67×10^{-32}	2.3	1.67×10^{-32}	2.1
60	408.8	2.15×10^{-31}	3.0	2.50×10^{-32}	4.7		
60	408.8	2.13×10^{-31}	1.6	2.55×10^{-32}	2.2	1.70×10^{-32}	1.9
80	321.2			1.19×10^{-32}	3.2	9.24×10^{-33}	2.7
100	271.8	6.39×10^{-32}	1.4	6.03×10^{-33}	2.3	5.43×10^{-33}	2.2
100	271.8	6.14×10^{-32}	3.3	6.49×10^{-33}	4.2		
120	242.1	4.00×10^{-32}	2.1	3.34×10^{-33}	4.9	3.80×10^{-33}	3.0
135	227.9	3.11×10^{-32}	1.9	2.01×10^{-33}	3.3	2.96×10^{-33}	2.5
$q^2=4.5$							
40	627.7	4.38×10^{-31}	2.1	3.59×10^{-32}	2.5	2.37×10^{-32}	2.5
40	627.7			3.63×10^{-32}	2.0	2.38×10^{-32}	1.7
50	511.1	2.73×10^{-31}	3.9	2.12×10^{-32}	4.1		
50	511.1	2.61×10^{-31}	1.8	2.28×10^{-32}	2.2	1.48×10^{-32}	1.9
60	434.5			1.41×10^{-32}	2.5	1.02×10^{-32}	2.2
60	434.5	1.76×10^{-31}	1.7	1.38×10^{-32}	2.1	1.03×10^{-32}	1.8
80	341.6			6.89×10^{-33}	4.5	5.39×10^{-33}	4.0
100	289.3	5.48×10^{-32}	2.1	3.44×10^{-33}	3.4	3.34×10^{-33}	3.6
135	242.7	2.69×10^{-32}	3.3	1.37×10^{-33}	6.1		
135	242.7	2.73×10^{-32}	1.9	1.25×10^{-33}	3.1	1.98×10^{-33}	2.5
$q^2=5.0$							
40	662.6	3.66×10^{-31}	1.2	2.04×10^{-32}	2.0	1.59×10^{-32}	1.9
40	662.6			2.09×10^{-32}	2.9	1.55×10^{-32}	3.3
40	662.6	3.79×10^{-31}	2.9	2.02×10^{-32}	3.2		
50	539.6	2.25×10^{-31}	1.1	1.28×10^{-32}	1.7	9.44×10^{-33}	1.7
60	458.9	1.49×10^{-31}	1.3	8.30×10^{-33}	2.5	6.49×10^{-33}	2.3
60	458.9			8.46×10^{-33}	2.9	6.33×10^{-33}	2.5
80	361.0			3.86×10^{-33}	3.3	3.49×10^{-33}	2.8
100	305.8	4.76×10^{-32}	2.1	2.08×10^{-33}	4.0	2.03×10^{-33}	3.3
100	305.8	4.72×10^{-32}	3.0	1.96×10^{-33}	5.1		
120	272.7	3.04×10^{-32}	1.7	1.11×10^{-33}	8.9	1.65×10^{-33}	4.2
120	272.7	3.00×10^{-32}	3.4	1.27×10^{-33}	6.5		
135	256.7	2.48×10^{-32}	3.8	6.95×10^{-34}	6.2		
$q^2=6.0$							
50	593.0	1.67×10^{-31}	1.5	4.76×10^{-33}	2.1	3.86×10^{-33}	1.8
100	337.0	3.57×10^{-32}	1.8	6.70×10^{-34}	6.3	9.98×10^{-34}	3.0
135	283.2	1.94×10^{-32}	2.0	2.75×10^{-34}	4.2	5.67×10^{-34}	3.5
$q^2=8.0$							
50	688.6	1.03×10^{-31}	1.5	4.49×10^{-34}	4.4	7.27×10^{-34}	3.6
80	462.7	3.71×10^{-32}	1.5	1.67×10^{-34}	5.5	3.03×10^{-34}	4.2
120	351.1	1.62×10^{-32}	1.9	6.12×10^{-35}	9.4	1.64×10^{-34}	6.9

nucleon, are all different due to the existence of a Coulomb repulsion in helium-3.

To evaluate $F_O(H^3)$ and $F_L(He^3)$ we need to know the charge form factors of the neutron and proton and to make an estimate of the values of the form factors $F_L(H^3)$ and $F_O(He^3)$. Although there is, at present, some disagreement between various measurements of the charge[16] form factor of the neutron, it is generally

TABLE II. Tritium and helium-3 form factors.

q^2 (F^{-2})	F_{ch}(H^3)	F_{mag}(H^3)	F_{ch}(He^3)	F_{mag}(He^3)	χ^2/N
1.0	0.622 ±0.007	0.653 ±0.022	0.567 ±0.004	0.676 ±0.075	1.09
1.5	0.503 ±0.007	0.475 ±0.015	0.431 ±0.004	0.479 ±0.046	1.54
2.0	0.387 ±0.007	0.379 ±0.012	0.329 ±0.004	0.385 ±0.031	2.42
2.5	0.312 ±0.006	0.312 ±0.008	0.258 ±0.003	0.291 ±0.020	2.16
3.0	0.267 ±0.005	0.242 ±0.006	0.209 ±0.002	0.203 ±0.014	2.19
3.5	0.215 ±0.004	0.199 ±0.005	0.1614±0.0017	0.167 ±0.010	1.59
4.0	0.175 ±0.004	0.167 ±0.004	0.1326±0.0015	0.128 ±0.009	1.64
4.5	0.137 ±0.003	0.139 ±0.003	0.1013±0.0010	0.118 ±0.005	1.10
5.0	0.118 ±0.004	0.109 ±0.005	0.0813±0.0012	0.093 ±0.008	2.27
6.0	0.0758±0.0041	0.0792±0.0032	0.0548±0.0015	0.0566±0.0056	3.45
8.0	0.0295±0.0039	0.0416±0.0018	0.0173±0.0010	0.0318±0.0026	0.63

accepted[17,18] that the value of $F_{ch}(n)$ is small (of the order of 0.1) in the range of q^2 of interest to the present experiment. Since the contribution to F_0(H^3) and F_L(He^3) of the terms involving $F_{ch}(n)$ is therefore small, we have decided to use the values of $F_{ch}(n)$ given by de Vries *et al.*[17] Also, we have made the approximations that

$$F_O(\text{He}^3)=F_L(\text{H}^3)=\tfrac{1}{2}(F_L(\text{He}^3)+F_O(\text{H}^3)),$$

which are acceptable because the form factors F_O(He^3) and F_L(H^3) enter only into the terms involving $F_{ch}(n)$.

With these assumptions we have solved the Eqs. (2) and (3) for F_0(H^3) and F_L(He^3). The results are given in Fig. 7 which shows that the form factor describing the spatial distribution of the protons in helium-3 decreases much more rapidly with increasing q^2 than the form factor describing the spatial distribution of the proton in tritium. This result might be expected, but at this time it is not possible to say to what extent the difference should be attributed to Coulomb repulsion, to meson exchange effects, or to a weaker nuclear force between the like particles. Also, in view of the inadequate state of the theory we do not think it meaningful to attempt to use these body form factors as a means of

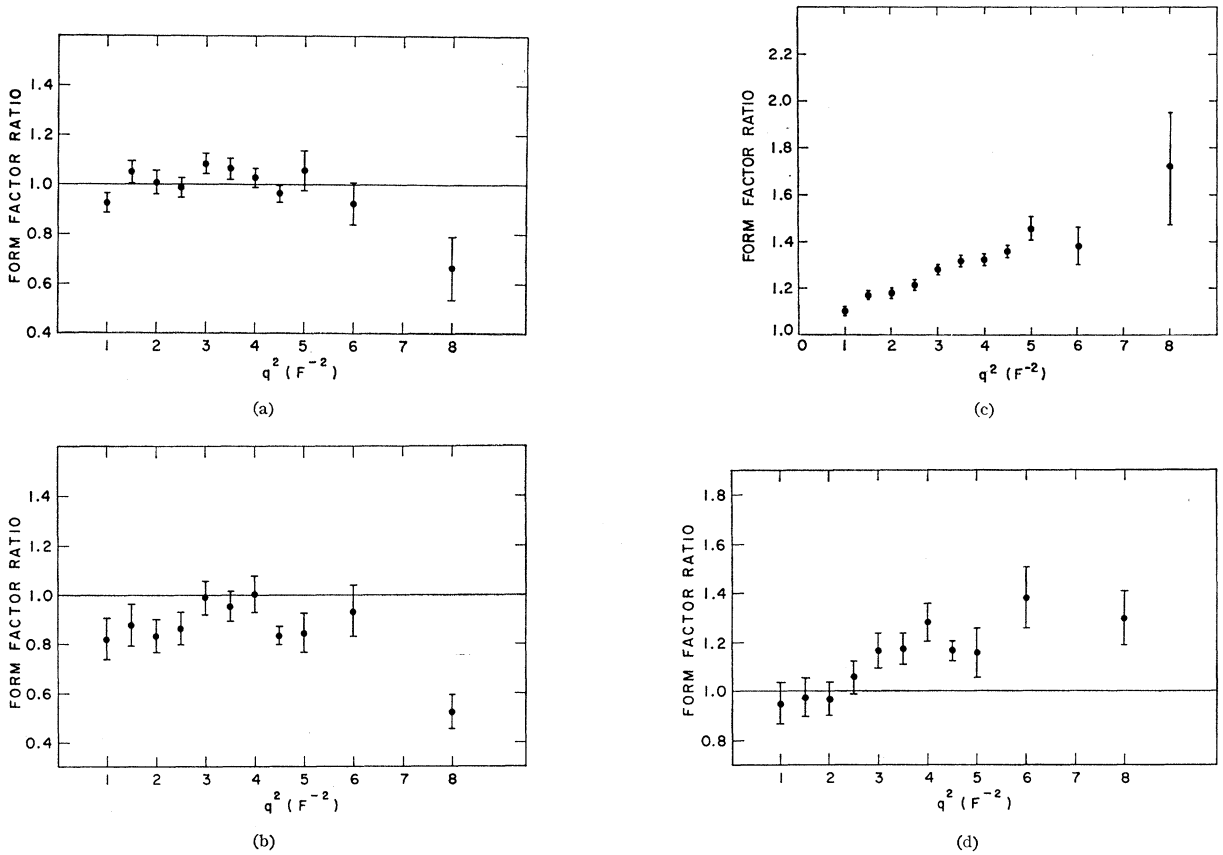

FIG. 6. The form factor ratios: (a) F_{ch}(H^3)/F_{mag}(H^3); (b) F_{ch}(He^3)/F_{mag}(He^3); (c) F_{ch}(H^3)/F_{ch}(He^3); (d) F_{mag}(H^3)/F_{mag}(He^3).

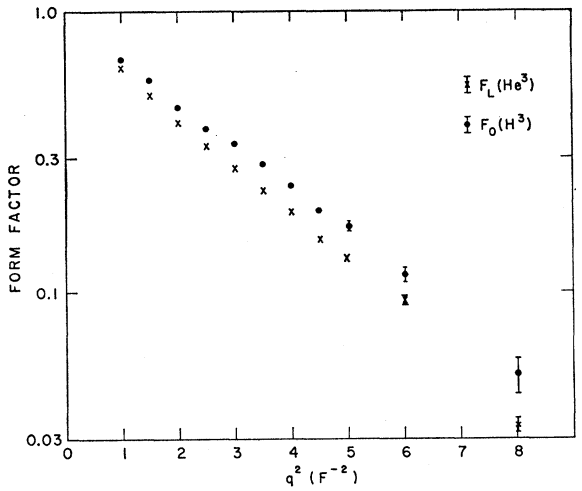

FIG. 7. Variation of the form factors $F_O(H^3)$ and $F_L(He^3)$ with four-momentum transfer squared.

determining the ground-state wave functions of the three-body nuclei.

NUCLEAR RADII

Model-independent determinations of the rms radii for the charge and magnetic moment distributions of tritium and helium-3 were made using both polynomial and exponential expressions for the form factors. In the case of the polynomial expression, $1-F(q^2)$ was plotted as a function of q^2 and the slope at the origin of a curve fitted by the method of least squares to these points was calculated. Both third- and fourth-order curves were used. Since the form factor can be expressed as $F(q^2)=1-\frac{1}{6}q^2a^2+$higher terms, the slope of $1-F(q^2)$ at the origin is

$$\left(\frac{d[1-F(q^2)]}{d(q^2)}\right)_{q^2=0}=\tfrac{1}{6}a^2,$$

from which the rms radius a can be determined.

To investigate model independence, the exponential case $-\ln F(q^2)$ was plotted as a function of q^2, and again the slope at the origin of a curve fitted by the method of least squares to these points was calculated. First-, second-, and third-order curves were used. Since, as before, the form factor can be expressed as $F(q^2)=1-\frac{1}{6}q^2a^2+$higher terms, it is clear that $-\ln F(q^2)=\frac{1}{6}q^2a^2+$higher terms for exponential curves of greater than first order, and the slope of $-\ln F(q^2)$ at the origin is

$$\left(\frac{d[-\ln F(q^2)]}{d(q^2)}\right)_{q^2=0}=\tfrac{1}{6}a^2$$

from which the rms radius a can be determined as in the polynomial case. Thus, each set of form factors was fitted by five curves. In addition to using all the experimental points, curves were fitted to all but the highest q^2 point, then all but the two highest q^2 points and so on, to find the best fit in each case and check the consistency of the results.

The values obtained from an averaging of the best results for the rms radii (in units of Fermis) are as follows:

$$a_{ch}(H^3)=1.70\pm0.05,\quad a_{ch}(He^3)=1.87\pm0.05,$$
$$a_{mag}(H^3)=1.70\pm0.05,\quad a_{mag}(He^3)=1.74\pm0.10.$$

The errors quoted are based on the range of the best results and the results appear to be model independent within the errors given. Note that $a_{ch}(H^3)$, $a_{mag}(H^3)$, and $a_{mag}(He^3)$ are nearly identical while $a_{ch}(He^3)$ is somewhat larger.

ACKNOWLEDGMENTS

We wish to gratefully acknowledge the assistance that we have received from the staffs of the Los Alamos Scientific Laboratory and Stanford University in helping us to overcome the special problems connected with the tritium and helium-3 targets. In particular, we are indebted to Don O. Coffin, Robert L. Mills, and Donald J. Sandstrom of Los Alamos for their help in the construction and filling of the target cells, and to Morris J. Engelke of Los Alamos and Carl Irwin of Stanford for their help on the health and safety problems of tritium. We are especially grateful to J. M. B. Kellogg and Norris E. Bradbury of the Los Alamos Scientific Laboratory for the enthusiastic support they gave to this joint project. We also wish to thank Hall Crannell most heartily for his assistance in applying a computer program to our data.